serval
serveur académique lausannois

UNIL | Université de Lausanne
Faculté de biologie
et de médecine

Impaired early visual response modulations to spatial information in chronic schizophrenia

Jean-François Knebel[a], **Daniel C. Javitt**[b], and **Micah M. Murray**[a,c,*]

[a]The Functional Electrical Neuroimaging Laboratory, Neuropsychology and Neurorehabilitation Service, Department of Clinical Neurosciences and Department of Radiology, Centre Hospitalier Universitaire Vaudois and University of Lausanne, Switzerland [b]Program in Cognitive Neuroscience and Schizophrenia, The Nathan S. Kline Institute for Psychiatric Research, Orangeburg, NY, USA [c]The Electroencephalography Brain Mapping Core, Center for Biomedial Imaging, Lausanne, Switzerland

Abstract

Early visual processing stages have been demonstrated to be impaired in schizophrenia patients and their first-degree relatives. The amplitude and topography of the P1 component of the visual evoked potential (VEP) are both affected; the latter of which indicates alterations in active brain networks between populations. At least two issues remain unresolved. First, the specificity of this deficit (and suitability as an endophenotype) has yet to be established, with evidence for impaired P1 responses in other clinical populations. Second, it remains unknown whether schizophrenia patients exhibit intact functional modulation of the P1 VEP component; an aspect that may assist in distinguishing effects specific to schizophrenia. We applied electrical neuroimaging analyses to VEPs from chronic schizophrenia patients and healthy controls in response to variation in the parafoveal spatial extent of stimuli. Healthy controls demonstrated robust modulation of the VEP strength and topography as a function of the spatial extent of stimuli during the P1 component. By contrast, no such modulations were evident at early latencies in the responses from patients with schizophrenia. Source estimations localized these deficits to the left precuneus and medial inferior parietal cortex. These findings provide insights on potential underlying low-level impairments in schizophrenia.

Keywords

Electroencephalography (EEG); electrical neuroimaging; event-related potential (ERP); visual evoked potential (VEP)

1. Introduction

Historically schizophrenia has been considered as primarily a disturbance in higher-order functions (Goldman-Rakic 1994; Goldberg TE & Gold JM 1995; Weinberger & Gallhofer

Corresponding author: Micah Murray, EEG Brain Mapping Core, Center for Biomedical Imaging, Radiology, CHUV, BH08.078, Rue du Bugnon 46, 1011 Lausanne, Switzerland, Tel : +41 21 3141321; Fax : +41 21 3141319, micah.murray@chuv.ch.

1997; Green 1998). More recently, there has been increasing interest in the contributions of early and low-level processing impairments. This has been most notable in the case of auditory processing where impairments in sensory gating and in mismatch negativity generation are well-documented (Umbricht et al. 2000; Umbricht et al. 2006; Lavoie et al. 2008). With regard to visual dysfunctions, a number of studies support there being deficits that more strongly impact functions associated with the magnocellular than parvocellular pathway (e.g Martínez et al., 2008; Coleman et al., 2009; Kiss et al., 2010). In particular, such deficits have been interpreted as indicative of disturbed spatial processing that in turn may lead to and/or appear conjointly with higher-level deficits (Butler & Javitt, 2005; Javitt, 2009)

Studies that have focused on the time course of these low-level visual processing impairments have found that visual evoked potentials (VEPs) over the initial 100ms (i.e. the P1 component) are impaired in patients with schizophrenia. A P1 deficit has not only been identified in chronic patients (Foxe et al. 2001; Doniger et al. 2002; Foxe et al. 2005), but also in first-degree relatives (Yeap et al. 2006). In particular, Foxe et al. 2005 demonstrated that this P1 deficit is not simply a shift in the amplitude of an otherwise intact process, but instead follows from a change in the configuration of the underlying brain network as revealed by topographic modulations in the VEP.

At present, however, it remains unknown whether this perturbed network is capable of exhibiting intact functional modulations in response to parametric variations in stimulus features. For example, Foxe et al. 2001 examined P1 amplitude in healthy controls and chronic patients with schizophrenia as a function of the number of pixels present in the visual display. While healthy controls exhibited an incremental modulation with increased numbers of pixels (and by extension stimulus energy), such was not observed in patients. Based on its topographic distribution (Foxe et al. 2001), estimated sources (Foxe et al. 2005), and relative sensitivity to luminance contrast (Butler et al. 2001) the P1 deficit in schizophrenic patients has been generally ascribed to impairments within dorsal visual stream structures. This proposition is in solid agreement with additional research demonstrating impairments in visuo-spatial functions in such patients (Cadenhead et al. 1998; Schwartz et al. 1999; Brenner et al. 2002; Butler et al. 2003). However, at present it remains unknown whether the P1 deficit obtained in VEP studies reflects impaired spatial processing per se or instead a more general diminution in visual processing/sensitivity.

The present study focused on early visual processing in chronic schizophrenia patients with the objective of determining whether impaired responses reflect impaired sensitivity to spatial features. Prior work from our group has shown that in healthy controls the P1 is sensitive to small (<1°) variations in the spatial eccentricity of parafoveally presented stimuli (Murray et al., 2002). Here, we compared VEPs from patients in response to such variations in the spatial eccentricity of stimuli that were oriented to form an illusory contour shape or not. Given that patients have been shown to exhibit intact sensitivity to illusory contour forms (Foxe et al. 2005), we could thus dissociate spatial from form-related processes.

2. Materials and Methods

2.1. Participants

A total of 16 individuals participated in this study. There were 8 chronic and medicated patients (all males; 2 left-handed), aged 36-47 years (mean±SD = 42±4 years) at the time of EEG recording and meeting DSM-IV criteria for schizophrenia. The control cohort included 8 individuals (all males; 1 left-handed), aged 25-53 years (mean±SD = 39±11 years) and with no history of or current neurological or psychiatric illness. There was no reliable

difference in the ages of the patient and control populations ($t_{(14)}$=0.725; p=0.481). All participants had normal or corrected-to-normal vision. These participants are a subset of those from our prior work (Foxe et al. 2005), which included 16 patients with schizophrenia and 17 healthy controls. Exclusion of data from 8 of the original 16 patients was due to poor signal quality in the VEPs when averaged according to the subset of stimuli described below. Data from control subjects were excluded to generate a cohort matched in size, age, and sex. Positive and Negative Symptoms Scale (PANSS) ratings were performed by a single rater, with factors defined according to White et al. (1997). At the time of testing, all patients were receiving antipsychotic medication. There was no evidence, however, for correlations between antipsychotic dose and any of the dependent measures evaluated in this study. Details regarding clinical evaluation and medication are provided in Table 1. Controls were free of psychiatric illness or symptoms by self-report using criteria from the SCID-NP (see Spitzer et al. 1992S), and all reported no history of alcohol or substance abuse.

2.2. Stimuli and Task

Participants were instructed to centrally fixate an array of Kanizsa-type (Kanizsa 1976) 'pacmen' inducers that were oriented in one of two manners to either form or not form an illusory shape ('IC' and 'NC' conditions, respectively). The timing of the stimuli and response window is detailed below. The inducers were circular (subtending 3° of visual angle in diameter) and appeared black on a gray background. Stimuli were presented on a CRT computer monitor (Iiyama Vision Master Pro 502, model no. A102GT) located 114cm away from the participant. Their task was to indicate whether they perceived a gray shape on top of the pacmen.

Five shapes were induced in the original study of Foxe et al. 2005 from which the present data come: square, circle, triangle, pentagon and star. In order to produce illusory shapes of the same maximal width and height (6° in either plane), the eccentricity of inducers varied slightly across shapes (cf. Table 1 in Murray et al. 2002). The analyses in the present study focused on VEPs to the square and circle as well as their corresponding configurations that were oriented so as to not induce the perception of an illusory shape. That is, both IC and NC configurations were analyzed. In the case of the square, the four inducers were centered at 4.25° eccentricity along 45° radii from central fixation. For the circle, the four inducers were located at 3° eccentricity along the horizontal and vertical meridians. The support ratio (i.e. the percentage of the perimeter of the illusory shape revealed by the inducers; Ringach & Shapley 1996) was 50% for the square and 64% for the circle. The surface area of the induced IC shapes was $36^{\circ 2}$ in the case of the square and $28.3^{\circ 2}$ in the case of the circle (Figure 1). Throughout this study, we refer to the IC and NC configurations of the square as "wide" and those of the circle as "narrow" (Figure 1). The reason for this choice is that studies in healthy controls have shown that early VEP responses to the square and circle (as well as their NC counterparts) differ due to the eccentricity of the inducers (Murray et al., 2002).

The timing of stimulus presentations during the course of a trial was such that each array of inducers appeared for 500ms, followed by a blank gray screen for 1000ms. Then a 'Y/N' response prompt appeared and remained on the screen until a response was made, allowing participants to fully control stimulus delivery. Another blank screen of 1000ms duration followed participants' responses. Subjects were instructed to press one button for a 'No' response, indicating that they did not perceive a gray shape 'pop-out' from the background, or a second button for a 'Yes' response, indicating that they perceived a gray shape on top of the inducers. IC and NC inducer configurations were randomly presented and were equally probable. Stimulus presentation and response collection were controlled using Neuroscan's STIM software and hardware. Subjects were encouraged to take breaks between blocks to maintain high concentration and prevent fatigue. Use of the response prompt was to displace

in time the motor responses with respect to the sensory VEP. Consequently, however, reaction time data were not analyzed.

2.3. EEG acquisition and pre-processing

Continuous EEG was acquired through Neuroscan Synamps (Neurosoft Inc. Sterling VA) from 64 Ag/AgCl electrodes (impedances <5kΩ, nose reference, 0.05 – 100Hz band pass filter, 500Hz sampling rate). For VEP calculation EEG epochs were time-locked to the presentation of inducer arrays and covered 100ms pre-stimulus and 500ms post-stimulus. Epochs with amplitude deviations in excess of ±80μV at any channel, with the exception of those labeled as 'bad' due to poor electrode-skin contact or damage, were considered artifacts and were excluded. Likewise, trials with blinks or other transients were excluded off-line based on vertical and horizontal electrooculograms. Data from 'bad' channels were interpolated using 3D splines (Perrin et al. 1987), and data were down-sampled to a 61-channel scalp montage used for source estimations. On average, 1 electrode was interpolated for control subjects (∈ [0,3]) and 3 were interpolated for patients (∈ [0,5]). Prior to group-averaging VEPs, data were band-pass filtered (0.1-60Hz), re-calculated to an average reference, and baseline corrected using the pre-stimulus interval. For each participant, 4 VEPs were calculated, following the 2 condition (IC, NC) × 2 eccentricity (wide, narrow) within subject design. The number of accepted sweeps per condition was ~110 for controls (∈ [54,197]) and ~ 70 for patients (∈ [30,124]).

2.4. EEG analyses

The analyses were performed using the Cartool software by Denis Brunet (http://brainmapping.unige.ch/Cartool.htm). This study followed a 2×2×2 mixed model design, using the within subjects factors of stimulus eccentricity (wide vs. narrow) and stimulus condition (IC vs. NC) and the between subjects factor of clinical status (patients vs. controls). Given the cohort size for each group, non-parametric statistics were used throughout. The repeated measures non-parametric F-test is a bootstrapping of the subjects on the one hand (taking with replacement the subject label) and permutation of the within subjects factors on the other. On each cycle we calculate for each randomization an F-value. Repeating this for 1000 cycles generates an empirical distribution of F-values from which a corresponding p-value can be obtained. This method has the advantage of keeping the intra-variance of the subjects and the only hypothesis is that our data represent the space that we would like to test. Unfortunately, this type of analysis does not readily allow for the calculation of effect size. Nor does the F-value itself (alongside its degrees of freedom) provide a direct indication of the statistically reliability of an effect/interaction, as one must instead consider it against the empirical distribution.

Effects were identified with a multi-step analysis procedure, which we refer to as electrical neuroimaging, examining reference-independent global measures of the electric field at the scalp (Michel et al. 2004; Murray et al. 2008). Briefly, electrical neuroimaging entails analyses of response strength and response topography to differentiate effects due to modulation in the strength of responses of statistically indistinguishable brain generators from alterations in the configuration of these generators (viz. the topography of the electric field at the scalp). Electrical neuroimaging analyses, being reference-independent, have several advantages over canonical waveform analyses. The statistical outcome with voltage waveform analyses will change with the choice of the reference electrode (Murray et al. 2008). Our conclusions are based solely on reference-independent global measures of the electric field at the scalp. In addition, we utilized the local auto-regressive average distributed linear inverse solution (LAURA; Grave de Peralta Menendez et al. 2001) to visualize and statistically contrast the likely underlying sources of effects identified in the VEPs.

Changes in the strength of the electric field at the scalp were assessed using global field power (GFP) from each participant and experimental condition (Lehmann and Skrandies, 1980; Koenig and Melie-Garcia, 2010). Values at each time point were compared with a repeated measures non parametric F-test, as above. To account for temporal auto-correlation, only effects persisting for at least 10ms were considered reliable (see Guthrie and Buchwald, 1991).

A K-means clustering analysis of the VEP topography at the scalp identified time periods of stable topography independent of VEP strength (data are normalized), which is a data-driven measure (Murray et al. 2008; Murray et al. 2009). The optimal number of topographies or 'template maps' that accounted for the group-averaged data set (i.e. the post-stimulus periods of all conditions from both patients and controls, collectively) was determined by a modified cross-validation criterion (Murray et al. 2008; Murray et al. 2009). The pattern of template maps identified in the group-averaged data across patients and controls was then statistically tested in the data of each individual participant, using spatial correlation to label each data point as better matching one or another template map. The output is a measure of relative map presence for each participant that is in turn submitted to a repeated measures non parametric F-test with the within subject factors of condition, eccentricity, and map as well as the between subjects factor of clinical status. This procedure reveals whether and when VEPs are more often described by one map versus another, and therefore whether different intracranial generator configurations are engaged.

We estimated the sources in the brain underlying the VEPs using a distributed linear inverse solution (ELECTRA) applying the local autoregressive average (LAURA) regularization approach to address the non-uniqueness of the inverse problem (Grave de Peralta Menendez et al. 2001; Grave de Peralta Menendez et al. 2004; Michel et al. 2004). The inverse solution algorithm is based on biophysical principles derived from the quasi-static Maxwell's equations; most notably the fact that independent of the volume conductor model used to describe the head, only irrotational and not solenoidal currents contribute to the EEG (Grave de Peralta Menendez et al. 2001; Grave de Peralta Menendez et al. 2004). As part of the regularization strategy, homogenous regression coefficients in all directions and within the whole solution space were used. LAURA uses a realistic head model, and the solution space included 3005 nodes, selected from a $6 \times 6 \times 6$ mm grid equally distributed within the gray matter of the Montreal Neurological Institute's average brain (courtesy of Grave de Peralta Menendez and Gonzalez Andino; http://www.electrical-neuroimaging.ch/). The head model and lead field matrix were generated with the Spherical Model with Anatomical Constraints (SMAC; Spinelli et al. 2000). As an output, LAURA provides current density measures; the scalar values of which were evaluated at each node. Prior basic and clinical research has documented and discussed in detail the spatial accuracy of this inverse solution (e.g. Grave de Peralta Menendez et al. 2004; Michel et al. 2004; Gonzalez Andino et al. 2005; Gonzalez Andino et al. 2005; Martuzzi et al. 2009). The time periods used for source estimations were determined from the above VEP analyses. Data from each subject and condition were first averaged as a function of time to generate a single data point. The inverse solution was then calculated for each of the nodes in the solution space. These data matrices were then submitted to repeated measures non-parametric F-test as above. The results of the source estimations were rendered on the MNI brain with the Talairach & Tournoux (1988) coordinates of the largest statistical differences indicated.

3. Results

3.1. Behavioral results

All participants readily performed the IC/NC discrimination task. Mean (s.d. indicated) accuracy for control subjects was 93±11.3%, 96±5.6%, 97±8.5%, and 98±5.6% for the

IC_wide, IC_narrow, NC_wide, and NC_narrow conditions, respectively. These values for patients were 97±5.6%, 92±6%, 97±5.17.0%, and 90±11.3%. Values from individual participants were statistically analyzed with a 2×2×2 repeated measures non-parametric F-test using the within subjects factors of stimulus eccentricity (wide vs. narrow) and stimulus condition (IC vs. NC) and the between subjects factor of clinical status (patients vs. controls). There were no main effects or interactions (all p>0.18). Thus, VEP effects are not readily explained by performance differences. These performance results also provide one level of evidence that all participants were able to allocate their attention to the stimuli.

3.2. Electrophysiological results

A first level of analysis of the VEP was performed using individual voltage waveforms, though we would remind the reader that our conclusions were based on reference-independent global measures detailed below. Responses from a parietal midline electrode (Pz) are shown in Figure 2 for controls and patients as a function of stimulus condition and stimulus eccentricity. Visual inspection of these waveforms suggests several effects. First, there appears to be a main effect of group, such that patients would appear to have a generally smaller P1 than controls (see also Foxe et al., 2005). Second, healthy controls appear to exhibit modulation over P1 VEP latencies as a function of stimulus eccentricity, whereas patients with schizophrenia do not. Third and by contrast, responses from both populations appear to modulate over N1 VEP latencies as a function of stimulus condition (i.e. as a function of illusory contour presence). These observations were statistically evaluated via a time-point by time-point 2×2×2 mixed model repeated measures non parametric F-test. There was a main effect of eccentricity over the 56-104ms and 124-150ms post-stimulus intervals. Responses were generally larger for the 'wide' than 'narrow' inducer arrays. There was also a main effect of stimulus condition over the 116-184ms, 352-446ms and 460-500ms post-stimulus intervals. Responses were generally larger to IC than NC stimuli. There was a main effect of group over the 58-100ms post stimulus interval, with generally stronger responses for controls than patients. Additionally, there was a significant group × stimulus eccentricity interaction over the 66-108ms post-stimulus interval and a group × stimulus condition interaction over the 256-274ms post-stimulus interval.

As described in the Materials and Methods, the VEP data were analyzed using electrical neuroimaging methods to independently identify modulations in response strength and response topography. Mean GFP waveforms are displayed in Figure 3 in response to each condition for each population separately. As above, visual inspection of these waveforms suggests that healthy controls exhibit modulation over P1 VEP latencies as a function of stimulus eccentricity, whereas patients with schizophrenia do not. By contrast, responses from both populations appear to modulate over N1 VEP latencies as a function of stimulus condition (i.e. as a function of illusory contour presence). These observations were statistically evaluated via a time-point by time-point 2×2×2 mixed model repeated measures non parametric F-test. There was a main effect of eccentricity over the 74-96ms and 108-138ms post-stimulus intervals, with generally stronger responses to 'wide' than 'narrow' inducer arrays. There was also a main effect of stimulus condition over the 126-170ms post-stimulus interval, with generally stronger responses to IC than NC stimuli. There was no evidence for a main effect of group at any latency, suggesting that clinical status did not lead to a general change in VEP strength. This also provides an argument against explanations in terms of attention differences or the fact that patients were medicated.

Of principal interest to the aims of the present study, there was a significant group × stimulus eccentricity interaction over the 84-94ms post-stimulus interval. To provide the reader with a sense of the consistency of the group × eccentricity interaction, GFP waveform

data from each participant are shown in Supplementary Figure S1. In order to better identify the basis of this interaction, additional 2×2 within subject repeated measures non parametric F-tests were performed as a function of time. In the case of healthy controls, there was a main effect of stimulus eccentricity over the 78-96ms, 118-130ms, and 168-184ms post-stimulus intervals. There was also a main effect of stimulus condition over the 124-156ms post-stimulus interval. In the case of patients with schizophrenia, there was a main effect of stimulus eccentricity over the 114-136ms interval. There was also a main effect of stimulus condition over the 144-160ms post-stimulus interval. Thus, controls but not patients exhibited robust modulation with stimulus eccentricity during the P1 period. We would add that there was also a significant interaction between group and stimulus condition over the 388-404ms post-stimulus interval. However, we do not discuss this effect in detail here for two main reasons. First, this effect is considerably subsequent to effects and interactions involving stimulus eccentricity. Second, this effect echoes that which we have previously reported in our original study (Foxe et al., 2005).

Modulations in response topography within and between groups were investigated using a cluster analysis. Across the concatenated dataset (i.e. the grand-average VEPs for the full 2×2×2 design), 13 template maps were identified that explained 96.06 % of the variance. Indistinguishable topographies were observed across groups, stimulus conditions, and stimulus eccentricities at all latencies, with the exception of the 54-108ms post-stimulus period (i.e. the P1 component). Over this time period, two maps were observed in the responses from healthy controls that differed between 'wide' and 'narrow' eccentricities irrespective of IC vs. NC stimulus condition. By contrast, all responses from patients with schizophrenia were described by a single map. These observations at the grand-average level were statistically examined at the single-subject level using a 2×2×2×2 repeated measures non-parametric F-test on the output of the fitting procedure described in Materials and Methods; the additional factor being map. This analysis revealed significant interactions between eccentricity and map (p=0.001) as well as between group, eccentricity, and map (p=0.01) see Figure 4. As above, to provide the reader with a sense of the consistency of the group × eccentricity interaction, fitting results from each participant are shown in Supplementary Figure S2. Because topographic differences forcibly follow from differences in the configuration of the underlying sources (Lehmann, 1987), this pattern of results demonstrates that patients and controls differ in the brain networks recruited to differentiate between wide and narrow stimulus eccentricities over the 54-108ms period.

Distributed source estimations were performed on single-subject data after first averaging the VEPs as a function of time over the 54-108ms post-stimulus interval. This period was selected based on the above topographic clustering analysis. For each node within the solution space we performed a 2×2×2 repeated measures non parametric F-test (clinical status × stimulus condition × stimulus eccentricity). We applied a p<0.01 threshold at the single-node level in conjunction with a 6-node spatial extent criterion. There was a significant clinical status × stimulus eccentricity interaction within two circumscribed brain regions (Figure 5). To label the location of these brain regions, we used a weighted mean across nodes (using 1-p-values) and selected the node with the maximal value within each region. The clinical status × stimulus eccentricity interaction was observed within Brodmann Areas 7/31 (i.e. left precuneus and medial inferior parietal cortex) and Brodmann Area 3 (i.e. left post-central gyrus). The basis for this interaction within each region was due to wide vs. narrow modulations in healthy controls, but not in chronic patients (Figure 5)

4. Discussion

The present findings deepen our understanding of early, low-level sensory processing impairments in patients with chronic schizophrenia. To date, general visual impairments

have been documented without also assessing whether such diminished responses also exhibited intact modulations with stimulus or task parameters. Here, we showed that the P1 deficit is not simply due to attenuated responses in patients. Rather, there was an interaction between spatial features of the stimuli and clinical status, such that patients failed to exhibit a P1 modulation as a function of stimulus eccentricity while controls exhibited larger and topographically distinct responses to widely distributed stimuli. Not only were P1 responses indistinguishable between wide and narrow stimulus eccentricities, but the VEP topography in patients was characterized by that accounting for responses to the narrow condition in healthy controls. That is, patients responded to both eccentricities as if they were "narrow". Source estimations further revealed that this impairment followed from diminished activity within parietal structures, consistent with models implicating magnocellular and/or dorsal visual stream processing impairments in schizophrenia. Importantly, the temporal resolution of VEP and electrical neuroimaging analyses revealed that patients did indeed exhibit sensitivity to spatial stimulus features at subsequent processing stages when control subjects also exhibited recursive treatment of this feature, ruling out explanations in terms of general insensitivity.

Prior studies have documented reduced P1 responses to visual stimuli not only in chronic patients (Foxe et al. 2001; Doniger et al. 2002; Foxe et al. 2005; Butler et al. 2007), but also in their first-degree relatives (Yeap et al. 2006). In the Yeap et al. 2006 study a substantial P1 reduction was demonstrated in response to isolated-check stimuli in both patients as well as their first-degree relatives compared to controls. These findings are suggestive of a potential endophenotype, though more recently Yeap et al. 2009 observed a similar impairment in patients with bipolar disorder. Thus, the specificity of the P1 reduction remains to be established. The present study, which we would emphasize is a more fine-grained analysis of a subset of the data in Foxe et al. (2005), highlights analytical methods that may assist in differentiating patient populations according to specific functional impairments and/or specific patterns of VEP modulations (e.g. topographic vs. strength) during the P1 component (or other periods) that in turn would reflect distinct neurophysiologic mechanisms and/or clinical states. Source estimations of effects in the present study revealed significant differences between healthy controls and chronic patients within the left precuneus and medial inferior parietal cortex as well as the left pre-central gyrus. On the one hand, the left-hemisphere laterality of this localization is also consistent with prior studies (Roemer et al., 1978; though see Butler et al., 2006). On the other hand, this localization is consistent with a deficit within the dorsal visual pathway (see also Sehatpour al., 2010). We would emphasize that replication of the present findings with a larger cohort as well as during earlier stages of schizophrenia will be important to establish potential biomarkers.

While sensitivity to the spatial eccentricity of the inducers was impaired over the P1 component, intact processing of this feature by chronic patients was indeed observed at subsequent processing stages. That is, main effects of stimulus eccentricity were observed in both groups over the 100-150ms post-stimulus interval both at the level of individual scalp electrodes (Figure 2) and also at the level of Global Field Power (Figure 3). Thus, impaired sensitivity to the spatial eccentricity of stimuli would appear to be delimited to early time periods. At later latencies (i.e. ~250ms and thereafter), by contrast, there was evidence for main effects of stimulus eccentricity in patients that were not evident in controls. One possibility is that such effects constitute a compensatory mechanism in patients for early spatial processing impairments. This possibility is particularly tempting in light of psychophysical evidence that patients are impaired in hierarchical processing of visual stimuli, favoring global over local percepts (e.g.Coleman et al. 2009). A speculative possibility is that compensatory mechanisms for early deficits that particularly effect

sensitivity to wider spatial distributions result in a subsequent hyper-sensitivity to spatially distributed information.

Several aspects of our findings speak against an explanation in terms of generally diminished attention or arousal in patients vs. controls. First, performance by the patients on the discrimination of the presence vs. absence of illusory contour stimuli was indistinguishable from that of controls, suggesting that patients were adequately engaged in the task and did not find it more (or less) demanding than control subjects. Second, the wide/narrow difference was not requisite to the task of illusory contour presence discrimination. Such being said, sensitivity to the spatial position and orientation of the inducer stimuli was (likely) necessary for accurate performance. Finally, our analyses revealed that while sensitivity to the wide/narrow distribution of inducers was not observed over the P1 period, it was indeed observed at subsequent time periods preceding the initial sensitivity to the presence vs. absence of illusory contours. This would suggest that any deficit is not general, but rather likely specific to early stages of spatial processing; though fully resolving this will require additional investigations. Plus, it will be informative to examine to what extent and in what manner factors like spatial attention impact patients' sensitivity to the spatial features of the stimuli. For example, it may be the case that early-latency deficits like that reported here persist even when attention (viz. task demands) is directed to the spatial distribution of the stimuli. By contrast, subsequent stages, which in the present paradigm were intact, might well become susceptible to impairments when spatial attention is also at play, given previous demonstrations of impaired attention-related functions in patients with schizophrenia (e.g. Schwartz et al. 2001).

An alternative explanation for the VEP modulation seen in control subjects is that the differences are due to the position of the inducers (in terms of their polar angle) rather to their spatial eccentricity. That is, the inducers defining the circle (as well as its NC counterpart) are located along the horizontal and vertical meridians, whereas those defining the square (and its NC counterpart) are located along the diagonals. Any VEP differences would therefore reflect this polar angle difference in stimulus position, rather than their eccentricity per se. If this were indeed the case, then the deficit reported here for patients with schizophrenia would be indicative of impaired processing of specific retinotopic positions – something to our knowledge that has yet to be documented (cf. Martínez et al. 2008 for retinotopic mapping data in patients). Nonetheless, we consider such an account unlikely because the present VEP modulations as a function of inducer eccentricity can be observed even when controlling for their position in terms of polar angle (Murray et al., 2002). Plus, the localization of the statistical differences in the source estimations observed in the present study within parietal structures provides a further argument against a purely retinotopic impairment in patients with schizophrenia.

Supplementary Material

Refer to Web version on PubMed Central for supplementary material.

Acknowledgments

References

Brenner CA, Lysaker PH, Wilt MA, O'Donnell BF. Visual processing and neuropsychological function in schizophrenia and schizoaffective disorder. Psychiatry Research. 2002; 111:125–136. [PubMed: 12374630]

Butler PD, Schechter I, Zemon V, Schwartz SG, Greenstein VC, Gordon J, Schroeder CE, Javitt DC. Dysfunction of early-stage visual processing in schizophrenia. American Journal of Psychiatry. 2001; 158:1126–1133. [PubMed: 11431235]

Butler PD, DeSanti LA, Maddox J, Harkavy-Friedman JM, Amador XF, Goetz RR, Javitt DC, Gorman JM. Visual backward-masking deficits in schizophrenia: relationship to visual pathway function and symptomatology. Schizophrenia Research. 2003; 59:199–209. [PubMed: 12414076]

Butler PD, Hoptman MJ, Nierenberg J, Foxe JJ, Javitt DC, Lim KO. Visual white matter integrity in schizophrenia. American Journal of Psychiatry. 2006; 163:2011–2013. [PubMed: 17074957]

Butler PD, Javitt DC. Early-stage visual processing deficits in schizophrenia. Current Opinion in Psychiatry. 2005; 18:151–157. [PubMed: 16639168]

Butler PD, Martinez A, Foxe JJ, Kim D, Zemon V, Silipo G, Mahoney J, Shpaner M, Jalbrzikowski M, Javitt DC. Subcortical visual dysfunction in schizophrenia drives secondary cortical impairments. Brain. 2007; 130:417–430. [PubMed: 16984902]

Cadenhead KS, Serper Y, Braff DL. Transient versus sustained visual channels in the visual backward masking deficits of schizophrenia patients. Biological Psychiatry. 1998; 43:132–138. [PubMed: 9474445]

Coleman MJ, Cestnick L, Krastoshevsky O, Krause V, Huang Z, Mendell NR, Levy DL. Schizophrenia patients show deficits in shifts of attention to different levels of global-local stimuli: evidence for magnocellular dysfunction. Schizophrenia Bulletin. 2009; 35:1108–1116. [PubMed: 19737806]

Doniger GM, Foxe JJ, Murray MM, Higgins BA, Javitt DC. Impaired Visual Object Recognition and Dorsal/Ventral Stream Interaction in Schizophrenia. Archives of General Psychiatry. 2002; 59:1011–1020. [PubMed: 12418934]

Foxe JJ, Doniger GM, Javitt DC. Early visual processing deficits in schizophrenia: impaired P1 generation revealed by high-density electrical mapping. Neuroreport. 2001; 12:3815–3820. [PubMed: 11726801]

Foxe JJ, Murray MM, Javitt DC. Filling-in in Schizophrenia: a High-density Electrical Mapping and Source-analysis Investigation of Illusory Contour Processing. Cerebral Cortex. 2005; 15:1914–1927. [PubMed: 15772373]

Goldberg, TE.; Gold, JM. Neurocognitive functioning in patients with schizophrenia: an overview. In: Kupfer, DJ., editor. Psychopharmacology, the fourth generation of progress. 1995. p. 1245-1257.

Goldman-Rakic PS. Working memory dysfunction in schizophrenia. Journal of Neuropsychiatry and Clinical Neurosciences. 1994; 6:348–357. [PubMed: 7841806]

Gonzalez Andino SL, Michel CM, Thut G, Landis T, Grave de Peralta R. Prediction of response speed by anticipatory high-frequency (gamma band) oscillations in the human brain. Human Brain Mapping. 2005; 24:50–58. [PubMed: 15593272]

Gonzalez Andino SL, Murray MM, Foxe JJ, de Peralta Menendez RG. How single-trial electrical neuroimaging contributes to multisensory research. Experimental Brain Research. 2005; 166:298–304.

Grave de Peralta Menendez R, Gonzalez Andino S, Lantz G, Michel CM, Landis T. Noninvasive localization of electromagnetic epileptic activity. I. Method descriptions and simulations. Brain Topography. 2001; 14:131–137. [PubMed: 11797811]

Grave de Peralta Menendez R, Murray MM, Michel CM, Martuzzi R, Gonzalez Andino SL. Electrical neuroimaging based on biophysical constraints. Neuroimage. 2004; 21:527–539. [PubMed: 14980555]

Green, MF. Schizophrenia from a neurocognitive perspective. Boston, MA: Allyn & Bacon; 1998.

Guthrie D, Buchwald JS. Significance testing of difference potentials. Psychophysiology. 1991; 28:240–4. [PubMed: 1946890]

Javitt DC. When doors of perception close: bottom-up models of disrupted cognition in schizophrenia. Annual Review of Clinical Psychology. 2009; 5:249–275.

Kanizsa G. Subjective contours. Scientific American. 1976; 234:48–52. [PubMed: 1257734]

Kiss I, Fábián A, Benedek G, Kéri S. When doors of perception open: visual contrast sensitivity in never-medicated, first-episode schizophrenia. Journal of Abnormal Psychology. 2010; 119:586–593. [PubMed: 20677847]

Koenig T, Melie-Garcia L. A method to determine the presence of averaged event-related fields using randomization tests. Brain Topography. 2010; 23:233–242. [PubMed: 20376546]

Lavoie S, Murray MM, Deppen P, Knyazeva MG, Berk M, Boulat O, Bovet P, Bush AI, Conus P, Copolov D, Fornari E, Meuli R, Solida A, Vianin P, Cuénod M, Buclin T, Do KQ. Glutathione precursor, N-acetyl-cysteine, improves mismatch negativity in schizophrenia patients. Neuropsychopharmacology. 2008; 33:2187–2199. [PubMed: 18004285]

Lehmann, D. Principles of spatial analysis. In: Gevins, AS.; Remond, A., editors. Handbook of electroencephalography and clinical neurophysiology, vol 1: methods of analysis of brain electrical and magnetic signals. Amsterdam: Elsevier; 1987. p. 309-54.

Lehmann D, Skrandies W. Reference-free identification of components of checkerboard-evoked multichannel potential fields. Electroencephalography and Clinical Neurophysiology. 1980; 48:609–621. [PubMed: 6155251]

Martínez A, Hillyard SA, Dias EC, Hagler DJ, Butler PD, Guilfoyle DN, Jalbrzikowski M, Silipo G, Javitt DC. Magnocellular pathway impairment in schizophrenia: evidence from functional magnetic resonance imaging. Journal of Neuroscience. 2008; 28:7492–7500. [PubMed: 18650327]

Martuzzi R, Murray MM, Meuli RA, Thiran J, Maeder PP, Michel CM, Grave de Peralta Menendez R, Gonzalez Andino SL. Methods for determining frequency- and region-dependent relationships between estimated LFPs and BOLD responses in humans. Journal of Neurophysiology. 2009; 101:491–502. [PubMed: 19005004]

Michel CM, Murray MM, Lantz G, Gonzalez S, Spinelli L, Grave de Peralta R. EEG source imaging. Clinical Neurophysiology. 2004; 115:2195–2222. [PubMed: 15351361]

Murray, MM.; De Lucia, M.; Brunet, D.; Michel, CM. Principles of Topographic Analyses for Electrical Neuroimaging. In: Handy, TC., editor. Brain Signal Analysis: Advances in Neuroelectric and Neuromagnetic Methods. MIT Press; 2009.

Murray MM, Brunet D, Michel CM. Topographic ERP analyses: a step-by-step tutorial review. Brain Topography. 2008; 20:249–264. [PubMed: 18347966]

Murray MM, Wylie GR, Higgins BA, Javitt DC, Schroeder CE, Foxe JJ. The spatiotemporal dynamics of illusory contour processing: combined high-density electrical mapping, source analysis, and functional magnetic resonance imaging. Journal of Neuroscience. 2002; 22:5055–5073. [PubMed: 12077201]

Perrin F, Bertrand O, Pernier J. Scalp current density mapping: value and estimation from potential data. IEEE Transactions in Biomedical Engineering. 1987; 34:283–288.

Ringach DL, Shapley R. Spatial and temporal properties of illusory contours and amodal boundary completion. Vision Research. 1996; 36:3037–3050. [PubMed: 8917767]

Roemer RA, Shagass C, Straumanis JJ, Amadeo M. Pattern evoked potential measurements suggesting lateralized hemispheric dysfunction in chronic schizophrenics. Biological Psychiatry. 1978; 13:185–202. [PubMed: 667227]

Schwartz BD, Maron BA, Evans WJ, Winstead DK. High velocity transient visual processing deficits diminish ability of patients with schizophrenia to recognize objects. Neuropsychiatry, Neuropsychology, and Behavioral Neurology. 1999; 12:170–177.

Schwartz BD, Tomlin HR, Evans WJ, Ross KV. Neurophysiologic mechanisms of attention: a selective review of early information processing in schizophrenics. Frontiers in Bioscience. 2001; 6:D120–134. [PubMed: 11171555]

Sehatpour P, Dias EC, Butler PD, Revheim N, Guilfoyle DN, Foxe JJ, Javitt DC. Impaired visual object processing across an occipital-frontal-hippocampal brain network in schizophrenia: an integrated neuroimaging study. Archives of General Psychiatry. 2010; 67:772–782. [PubMed: 20679585]

Spinelli L, Andino SG, Lantz G, Seeck M, Michel CM. Electromagnetic inverse solutions in anatomically constrained spherical head models. Brain Topography. 2000; 13:115–125. [PubMed: 11154101]

Spitzer RL, Williams JB, Gibbon M, First MB. The Structured Clinical Interview for DSM-III-R (SCID). I: History, rationale, and description. Archives of General Psychiatry. 1992; 49:624–629. [PubMed: 1637252]

Talairach, J.; Tournoux, P. Thieme. Co-planar stereotaxic atlas of the human brain. New York: 1988.

Umbricht D, Schmid L, Koller R, Vollenweider FX, Hell D, Javitt DC. Ketamine-induced deficits in auditory and visual context-dependent processing in healthy volunteers: implications for models of cognitive deficits in schizophrenia. Archives of General Psychiatry. 2000; 57:1139–1147. [PubMed: 11115327]

Umbricht DSG, Bates JA, Lieberman JA, Kane JM, Javitt DC. Electrophysiological indices of automatic and controlled auditory information processing in first-episode, recent-onset and chronic schizophrenia. Biological Psychiatry. 2006; 59:762–772. [PubMed: 16497277]

Weinberger DR, Gallhofer B. Cognitive function in schizophrenia. International Clinical Psychopharmacology. 1997; 12 4:S29–36. [PubMed: 9352344]

Yeap S, Kelly SP, Reilly RB, Thakore JH, Foxe JJ. Visual sensory processing deficits in patients with bipolar disorder revealed through high-density electrical mapping. Journal of Psychiatry & Neuroscience. 2009; 34:459–464. [PubMed: 19949722]

Yeap S, Kelly SP, Sehatpour P, Magno E, Javitt DC, Garavan H, Thakore JH, Foxe JJ. Early visual sensory deficits as endophenotypes for schizophrenia: high-density electrical mapping in clinically unaffected first-degree relatives. Archives of General Psychiatry. 2006; 63:1180–1188. [PubMed: 17088498]
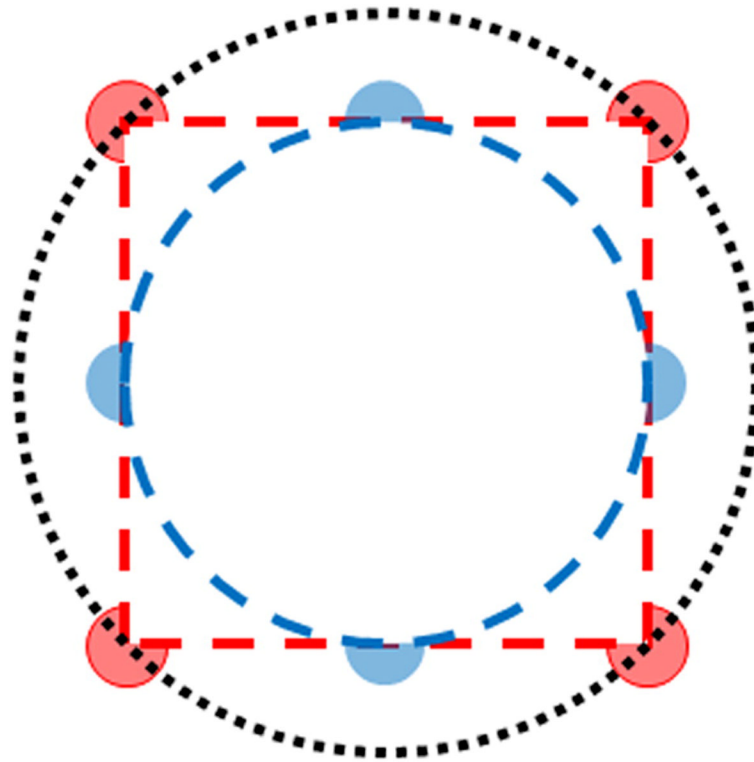
Figure 1.
Schematic of the relative eccentricity of the stimuli. For simplicity, only the stimulus orientations forming an illusory contour shape are shown. The wide eccentricity is shown in red. The narrow eccentricity is shown in blue.
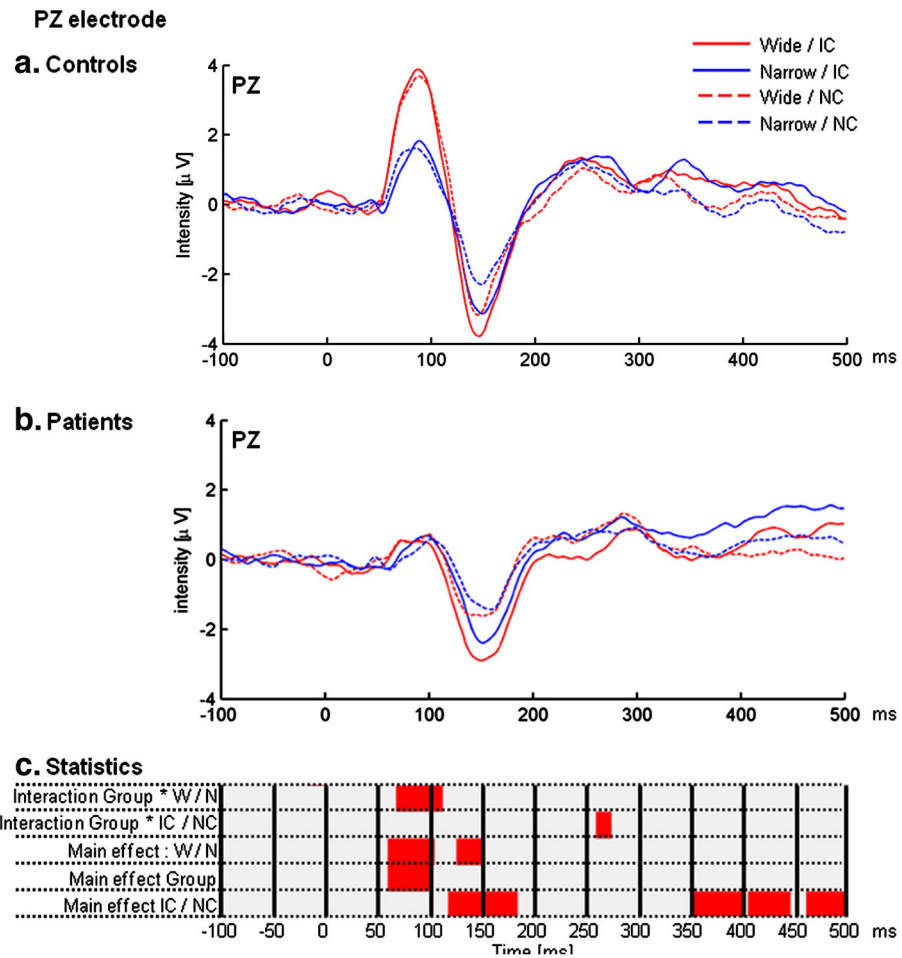
PZ electrode

Figure 2.
Exemplar group-average VEPs from healthy controls (panel a) and chronic patients with schizophrenia (panel b) at a parietal midline scalp site (Pz). In these plots the solid lines represent the illusory contour (IC) stimulus condition and the dotted lines the non-illusory contour (NC) stimulus condition. Red lines refer to the wide stimulus eccentricity and blue to the narrow stimulus eccentricity. Panel c displays the results of a time-point by time-point non-parametric F-test on the VEP at electrode Pz (alpha ≤0.05; temporal criterion of at least 6 contiguous time-points).
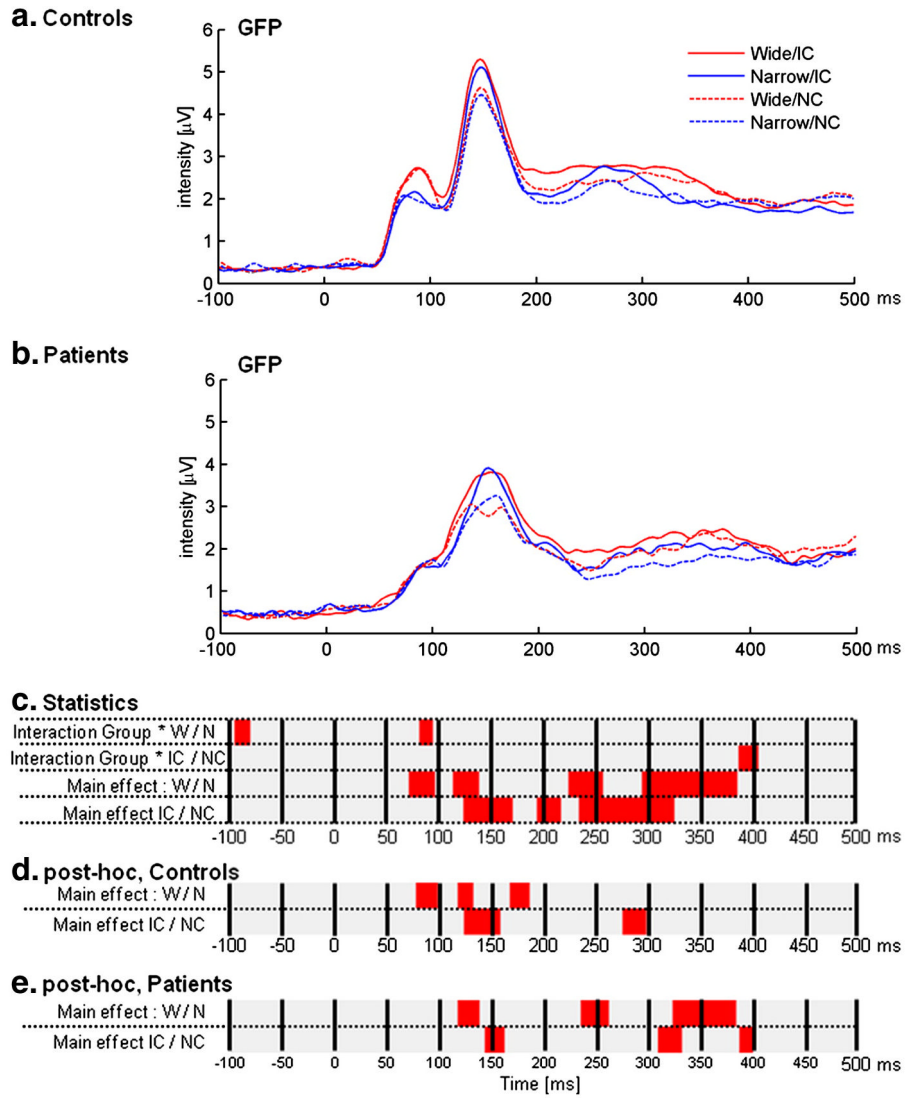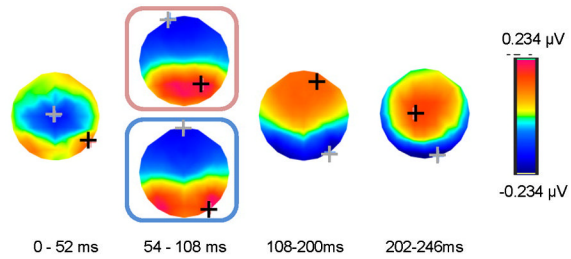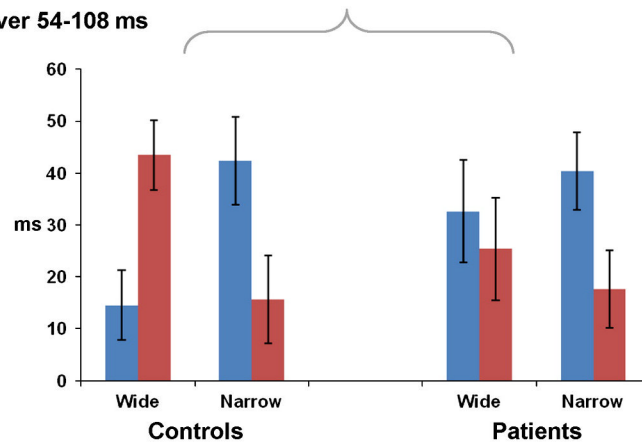
Figure 3.
Group-average global field power (GFP) waveforms from healthy controls (panel a) and chronic patients with schizophrenia (panel b). Conventions for the plots are identical to those in Figure 2. Panel c displays the results of a time-point by time-point non-parametric F-test on the GFP (alpha ≤0.05; temporal criterion of at least 6 contiguous time-points). Panels d and e display the post-hoc analyses on each group using the same criteria as in panel c.

Figure 4.
Panel a displays the results of the topographic cluster analysis of the group-averaged VEPs from both patients and controls. Over the initial ~250ms post-stimulus period, 4 topographies were identified in the group-averaged dataset. Two of these were observed over the 54-108ms post-stimulus period and were in turn used for single-subject fitting (see Materials and Methods for details). Panel b displays the results of the single-subject fitting analysis wherein both of the two topographies identified over the 54-108ms was spatially correlated with the instantaneous VEP. The bar graph shows the mean amount of time (over the 54-108ms post-stimulus interval) labeled with each topography (s.d. indicated) as a function of each cohort and stimulus eccentricity (i.e. data were collapsed across stimulus conditions for display purposes).
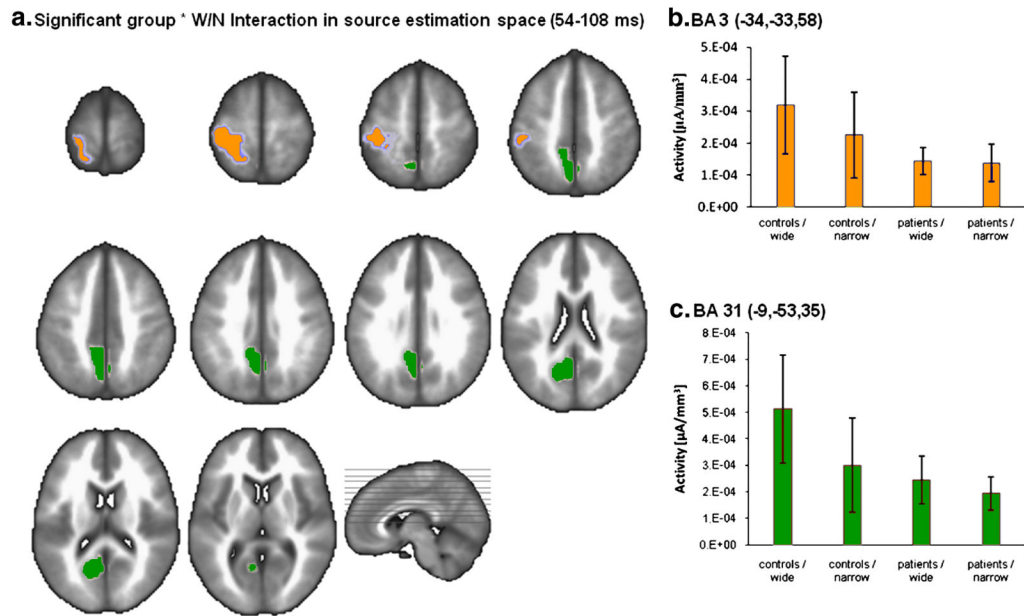
a. Significant group * W/N Interaction in source estimation space (54-108 ms)

b. BA 3 (-34,-33,58)

c. BA 31 (-9,-53,35)

Figure 5.
Source estimation analyses. Panel a depicts the loci within the source estimation space that exhibited a significant group * stimulus eccentricity interaction (non-parametric F-test). This test was performed after first averaging the VEPs from each condition and group as a function of time (54-108ms) to obtain a single vector per participant and condition that was in turn submitted to the source estimation and statistically analyzed. Two clusters were identified, which for clarity are colored orange and green. Panels b and c display the mean (s.d. indicated) scalar values within the cluster and across subjects and stimulus conditions. The coordinates shown are according to the Talairach and Tournoux (1988) atlas. Brodmann areas (BA) are likewise indicated. In both clusters, controls exhibited a significant difference between wide and narrow stimulus eccentricities, whereas patients did not.

Table 1
Demographic and Clinical Characteristics of Schizophrenia Patient Group (*N*=8)

Diagnosis: Schizophrenia/Schizoaffective Disorder	8/0
Neuroleptics: Atypical/Typical/Both	8/0/0
Chloropromazine (CPZ)-equivalent±SD, daily	1056.13±378.70
Clinical Global Impressions (CGI)±SD	4.25±0.46
Education±SD, y	11.14±3.34
Illness Duration±SD, y	17.88±6.27
Intelligence Quotient (IQ)±SD	96.0±9.32
Laterality Quotient±SD	0.62±0.70
PANSS: Positive Symptoms±SD	12.13±5.14
Negative Symptoms±SD	21.13±5.89
Autistic Preoccupation±SD	13.25±3.28
Activation±SD	6.88±2.03
Dysphoria±SD	11.38±2.26